Testing the Pattern of AKT Activation by Variational Parameter Estimation

DANIEL KASCHEK[1]**, FRAUKE HENJES**[2]**, MAX HASMANN**[3]**, ULRIKE KORF**[4]**, AND JENS TIMMER**[1]

[1]Institute of Physics, Freiburg University, Germany
[2]Life Technologies AS, Oslo, Norway
[3]Roche Diagnostics GmbH, Penzberg, Germany
[4]German Cancer Research Center, Heidelberg, Germany (Dr. Ulrike Korf is deceased.)

CORRESPONDING AUTHOR: D. KASCHEK (daniel.kaschek@physik.uni-freiburg.de)

ABSTRACT   Dynamic modeling has become one of the pillars of understanding complex biological systems from a mechanistic point of view. In particular, ordinary differential equations are frequently used to model the dynamics of the interacting states, e.g., molecular species in cell signaling pathways. The equations typically contain many unknown parameters, such as reaction rates and initial conditions, but also time-dependent parameters, i.e., input functions driving the system. Both are *a priori* unknown and need to be estimated from experimental, time-resolved data. Here, we discuss an application of indirect optimal control methods for input estimation and parameter estimation in the *mammalian target of rapamycin* (mTOR) signaling. Whereas the direct identification and quantification of different active mTOR complexes, e.g., *mTOR complex* 2 (mTORC2), is only possible by highly challenging experiments, the mathematical framework allows to reconstruct its dynamics by solving an appropriate Euler–Lagrange equation based on Pontryagin's maximum principle. The inherently large search space underlying this approach allows to test specific biological hypotheses about the activation of *protein kinase B* (AKT) by mTORC2 and to reject an alternative model with high statistical power. Hereby, we identify a minimal model that has AKT threonine phosphorylation as a prerequisite for serine phosphorylation by mTORC2. Based on this model, the activation of mTORC2 is predicted to be inhibited by drugs, targeting the receptors of the ERBB receptor family.

INDEX TERMS   Cancer, optimal control, parameter estimation.

I. INTRODUCTION

Input estimation and parameter estimation in ordinary differential equations (ODEs) are two sides of the same medal even though the dimensionality of the search space is finite for parameter estimation and infinite for input estimation. To determine both jointly, input functions can be finitely parameterized, e.g., using a finite set of basis functions. This is the principle of direct optimal control methods. Alternatively, an indirect method can be employed, where parameters are integrated into the ODE as (constant) states and the optimality condition derived from Pontryagin's maximum principle must be satisfied.

Both the methods have their advantages and disadvantages. Nowadays, direct methods have become very popular due to their robustness and applicability to large scale problems. On the other hand, indirect methods have shown to yield more precise results in some applications and be less affected by "pseudominima" as being generated by direct methods; see [1] and [2] for a comparison of direct and indirect methods and [3] for a more general overview.

In recent years, biological systems and biomedical questions have more and more prompted the interest of theoreticians. Their ideas have led to the applications of control theory in biology [4], [5]. Dynamic modeling by ODEs has become a wide-spread technique to analyze and understand the mechanisms of complex biological systems [6], [7]. On the other hand, maximum-likelihood estimation and likelihood theory provide a solid statistical framework for uncertainty analysis [8], identifiability analysis [9], and model selection [10]. However, combining maximum-likelihood with optimal control methods is not straightforward. In an earlier work [11], we have shown that the cost functional

$$\phi[u] = \int (x[u] - x^D)^2 + (u - u^D)^2 \mathrm{d}t$$

with ODE states x, input functions u, and the corresponding data functions x^D and u^D can be employed for uncertainty analysis by the profile-likelihood method when choosing appropriate weighting functions for the residuals $\mathrm{res}_x = x - x^D$ and $\mathrm{res}_u = u - u^D$. Thereby, we coupled an indirect

optimal control method based on the Euler–Lagrange equation of input estimation with maximum-likelihood theory and gave it statistical meaning.

In this letter, we focus on applying the indirect, variational method used in [11] to answer a biological question in the context of mammalian target of rapamycin (mTOR) signaling, combining the advantages of variational calculus, and statistical interpretation.

II. METHODS
Let

$$\dot{x} = f(x, u, p) \tag{1}$$

be a dynamic system defined on the time interval $I = [0, T]$ with states $x \in C^{\infty}(I, \mathbb{R}^n)$, inputs $u \in C^{\infty}(I, \mathbb{R}^m)$, and parameters $p \in \mathbb{R}^{\ell}$. Furthermore, let $\{x(t_i)^D\}_{i=1,\ldots,n_D}$ be the measurements of the states x at times t_i with uncertainties $\{\sigma_i\}_{i=1,\ldots,n_D}$. The measurements are translated into time-continuous data and weighting functions

$$x^D : t \longmapsto \mathrm{spline}\big(t \,|\, t_i, x_i^D\big) \tag{2}$$

$$w_x^D : t \longmapsto \sum_i \frac{\alpha_i}{\sqrt{2\pi\tau^2}} e^{-\frac{(t-\tau)^2}{2\tau^2}} \frac{1}{\sigma_i \odot \sigma_i} \tag{3}$$

where $\odot$ denotes the elementwise multiplication, spline($\cdot$) represents an interpolation spline, τ^2 is the variance of the Gaussians employed for extending the statistically motivated $(1/\sigma^2)$-weighting over the time axis, and the α_i values are normalization factors compensating the finite size of the interval I. The case of unobserved states corresponds to $w^D \equiv 0$.

Without loss of generality let us assume that u is part of the measured quantities. Thus, it is treated analogously to x. Consequently, the functional to be minimized reads

$$\phi[u] = \int_I \left[\sqrt{w_x^D} \odot (x[u] - x^D)\right]^2 + \left[\sqrt{w_u^D} \odot (u - u^D)\right]^2 \mathrm{d}t \tag{4}$$

and the first variation $\delta\phi$ can be expressed as

$$\delta\phi|_u = 2 \int_I \nabla_u f^* a + w_u^D \odot (u - u^D) \mathrm{d}t \cdot \delta u \tag{5}$$

where $*$ denotes the transpose and $\nabla_u f$ is the Jacobian of f with respect to u. The elements of the function $a \in C^{\infty}(\mathbb{R}, \mathbb{R}^n)$ are the adjoint sensitivities, satisfying the equations

$$\begin{aligned} \dot{a} &= -\nabla_x f^* a - w_x^D \odot (x - x^D) \quad a(T) = 0 \\ \dot{x} &= f(x, u, p) \qquad\qquad\qquad\quad x(0) = x_0. \end{aligned} \tag{6}$$

Beyond the contributions from u, the first variation $\delta\phi$ is also affected by changes δp in the parameters and δx_0 in the initial state values. All contributions together with the stationarity condition are collected in the following equations:

$$2 \cdot a(0) \cdot \delta x_0 = 0 \quad \text{(initial values)} \tag{7}$$

$$2 \int_I a^* \nabla_p f|_{\hat{p}} \mathrm{d}t \cdot \delta p = 0 \quad \text{(parameters)} \tag{8}$$

$$\big(\nabla_u f^* a + w_u^D \odot (u - u^D)\big) \cdot \delta u = 0 \quad \text{(input).} \tag{9}$$
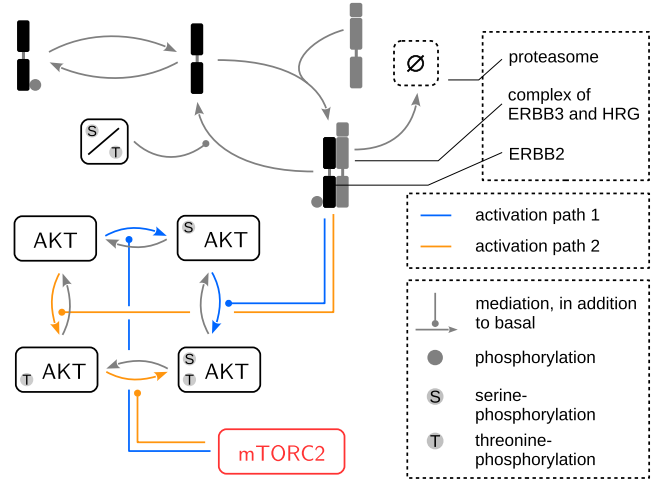
FIGURE 1. Pathway diagram. AKT threonine phosphorylation and serine phosphorylation are mediated by ERBB receptor phosphorylation and mTORC2. Principally, the two AKT phosphorylation steps can occur in both orders, denoted as activation paths 1 and 2. These present the two model hypotheses employed for model selection.

Equation (6) highlights that the original ODE has become a boundary value problem. Plugging (9) into (6) yields the Euler–Lagrange equations of input estimation, which return the optimal trajectories (x, a, u) for fixed parameters p and initial values x_0. The gradient expressions, (7) and (8), are used for successive optimization based on a trust-region algorithm with SR1 update to approximate the Hessian [12].

III. RESULTS
Variational parameter estimation is applied to the mTOR signaling pathway, a pathway being in the focus of cancer research due to its major role for cell survival and proliferation. One of its key players is AKT exerting its downstream activity by two phosphorylation sites: threonine (T308) and serine (S473). The threonine site is phosphorylated by a cascade from the receptor level via *phosphoinositide 3-kinase* (PI3K) and *phosphoinositide-dependent kinase-1* (PDK1). In contrast, the serine site is phosphorylated by mTOR complex 2 (mTORC2), which is modeled as an unknown input function to be determined by the variational approach.

The cell line employed for this letter is the SKBR3 breast cancer cell line. In order to stimulate downstream signaling, the cells were stimulated for 60 min with *heregulin* (HRG), an ERBB3 ligand, which induces dimer formation between ERBB3 and ERBB2 and thus activates PI3K and PDK1. Dimer formation, phosphorylation, and levels of mTORC2 can be affected by different anticancer drugs. In this letter, cells were treated with pertuzumab, erlotinib, and a combination of both at the time point 0 min. After 60 min, cells were stimulated with HRG, in addition to the drug, being still present in the system. These treatments represent the different experimental conditions. For a full specification of materials and methods, see [13].

An abstraction of the mTOR signaling pathway is shown in Fig. 1. The model comprises basal phosphorylation of the ERBB2 receptor as well as HRG-induced phos-
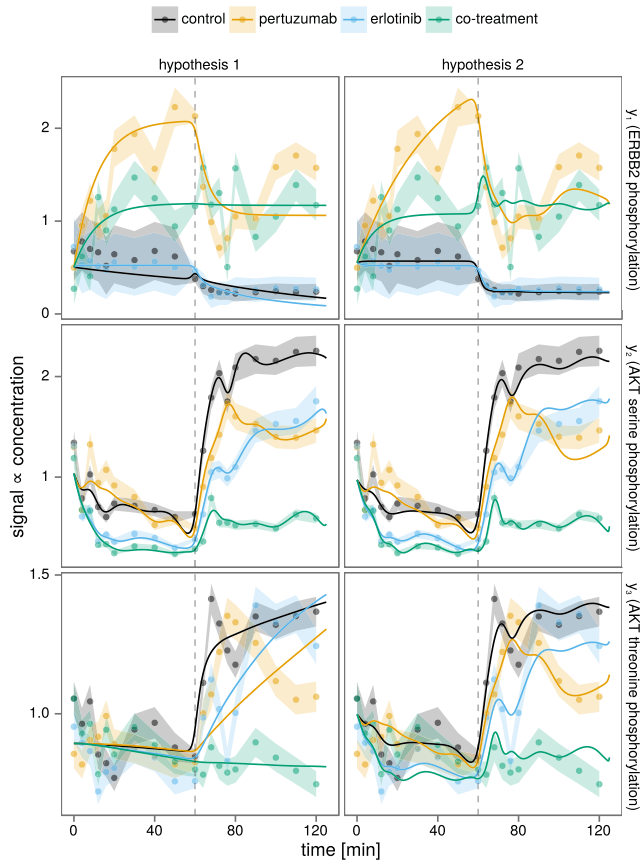
FIGURE 2. Observed states. Experimental data of ERBB2 and AKT phosphorylation sites were employed for functional parameter estimation. Different time courses obtained for untreated control cells as well as cells treated with pertuzumab, erlotinib, or both drugs simultaneously are visualized by different colors. Two activation path hypotheses were tested, shown in columns, resulting in significantly different model predictions.

phorylation of ERBB2 by dimer formation with ERBB3. The phosphorylated dimer is subject to two inactivation processes. First, dephosphorylation is controlled by a negative feedback of downstream targets and, thereby, occurs proportional to AKT phosphorylation. Second, the dimer is degraded by the proteasome, potentially shifting the steady state of receptor phosphorylation. Serine phosphorylation and threonine phosphorylation of AKT are mediated by the input state mTORC2 and the active receptor dimer, respectively. Depending on the order of the two phosphorylation steps, the AKT protein takes a different activation path, denoted as paths 1 (blue) and 2 (orange). Even if both the paths coexisted in the cells, the importance of each path could be assessed by concentrating on one pathway at a time: for hypothesis 1, all reaction rate parameters corresponding to path 2 are set to zero whereby activation path 2 is switched off in the model. Accordingly, for hypothesis 2, activation path 1 is switched off. See [14, Secs. 1 and 2] for the model equations and a full specification of the parameters.

Both the model hypotheses were tested with the same experimental data, i.e., relative values of ERBB2 phospho-

rylation (y_1), AKT serine phosphorylation (y_2), and AKT threonine phosphorylation (y_3) for the four experimental conditions. Based on the model structure, the observation function reads

$$y_1 = (pERBB2 + pERBB2 * ERBB3 * HRG)/s_1$$
$$y_2 = (pS\text{-}AKT + pSpT\text{-}AKT)/s_2 \qquad (10)$$
$$y_3 = (pT\text{-}AKT + pSpT\text{-}AKT)/s_3$$

where "p" denotes phosphorylation, "S" and "T" refer to serine and threonine, and "∗" indicates complex formation. Without loss of generality, the scaling factors satisfy $s_1 = s_2 = 1$. For each hypothesis, 500 fits determining rate constants, initial conditions, and the mTORC2 input were started from different points in parameter space to control convergence to the global optimum. See [14, Sec. 3] for more details. The fits with the lowest objective value, one for each hypothesis, are shown in Fig. 2. Each panel shows four measured time courses corresponding to the different experimental conditions and visualized as dots with 1σ error bands. The predictions by the fitted models are shown as solid lines. For both the hypotheses, ERBB2 phosphorylation and AKT serine phosphorylation are accurately described. However, the transient AKT threonine phosphorylation observed after pertuzumab treatment can only be explained by hypothesis 2. The free choice of an mTORC2 input function is fully utilized for hypothesis 1 to describe the course of AKT serine phosphorylation at the cost of a mismatch of threonine phosphorylation.

Both the hypotheses generate significantly different predictions on the dynamics of the unobserved states, i.e., for the reconstructed input course of mTORC2 and the internal dynamic states (see Fig. 3). According to hypothesis 1 [Fig. 3(a)], erlotinib does not inhibit mTORC2 formation, whereas pertuzumab has a slight inhibitory effect on mTORC2, which is not further increased by the cotreatment. In contrast, assuming hypothesis 2 [Fig. 3(b)], both the drugs, pertuzumab and erlotinib, inhibit mTORC2 formation and the most effective inhibition occurs upon cotreatment with both the drugs. This pattern has already been reported for other downstream targets, e.g., *mitogen-activated protein kinase* (ERK) [13].

Based on the model predictions for the four AKT states as shown in Fig. 3(c), hypothesis 1 corresponds to a very low ratio of doubly versus singly phosphorylated AKT. Thereby, the observed serine phosphorylation is exclusively explained by pS-AKT, whereas pSpT-AKT corresponds to the observed threonine phosphorylation. In contrast, hypothesis 2 favors a constellation, where pT-AKT provides a rather constant contribution of threonine phosphorylation, featuring a modest drop upon stimulation with HRG. Single phosphorylated AKT and double phosphorylated AKT exist in similar proportions, where the double phosphorylated form, pSpT-AKT, exhibits a larger fold-change to HRG stimulation.

The persistence of these results was verified by an observability analysis based on the 500 fits per hypothesis, see [14, Sec. 4].
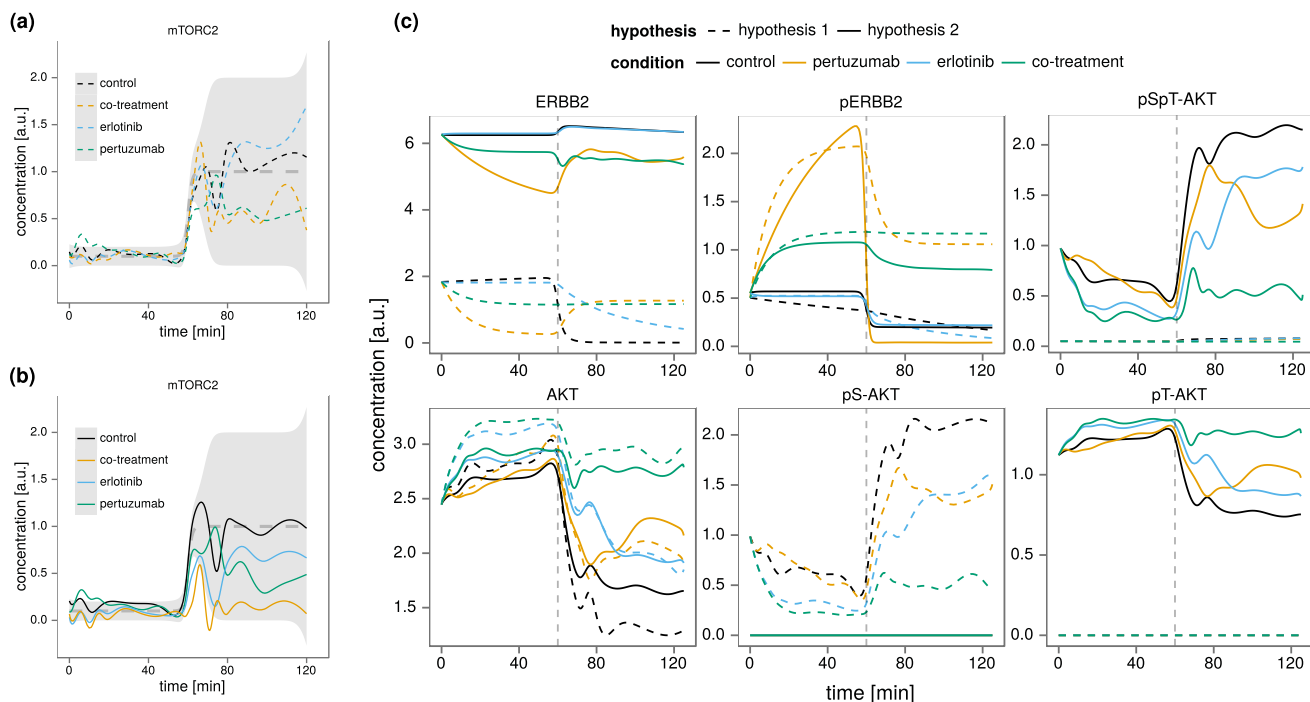
FIGURE 3. Unobserved states. The model makes distinct predictions for the two activation path hypotheses (line type) and different experimental conditions (colors). (a) and (b) Input estimation by the variational approach employs prior information about the dynamics and uncertainty of mTORC2, being represented by the gray dashed line and the shaded area. (c) Assumptions about the activation paths directly affect the pS-AKT and pT-AKT levels and eventually lead to distinct model predictions for the remaining states.

IV. CONCLUSION

Variational parameter estimation was applied to analyze and test two activation path hypotheses about mTOR signaling in the breast cancer cell line SKBR3. The analysis shows that serine phosphorylation as prerequisite for threonine phosphorylation, hypothesis 1, is in contradiction with the AKT threonine phosphorylation data and is therefore rejected. In contrast, threonine phosphorylation as a prerequisite for serine phosphorylation, hypothesis 2, explains the experimental data at such a level that the improvement obtained for the overarching model, featuring coexistence of both the paths, would not be significant. Based on our model for hypothesis 2, the anticancer drugs, pertuzumab and erlotinib, are predicted to inhibit mTORC2 formation and, thereby, reduce the levels of double phosphorylated AKT. This effect is highly enforced by cotreatment with both the drugs. Although our approach combining indirect optimal control methods and trust-region elements is limited to a certain model size, we see the advantage that it guarantees a huge search space for possible input course solutions. Possible misspecification of the input by a finite-dimensional parameterization is automatically avoided. Thereby, a highly stringent assessment of competing hypotheses is enabled, and allows the rejection of wrong model hypotheses not only over a large range of parameter values but also over a large class of input functions.

REFERENCES

[1] O. von Stryk and R. Bulirsch, "Direct and indirect methods for trajectory optimization," *Ann. Oper. Res.*, vol. 37, no. 1, pp. 357–373, Dec. 1992.

[2] K. Hatz, J. P. Schlöder, and H. G. Bock, "Estimating parameters in optimal control problems," *SIAM J. Sci. Comput.*, vol. 34, no. 3, pp. A1707–A1728, 2012.

[3] J. T. Betts, *Practical Methods for Optimal Control and Estimation Using Nonlinear Programming*, vol. 19. Philadelphia, PA, USA: SIAM, 2010.

[4] D. Lebiedz, S. Sager, H. Bock, and P. Lebiedz, "Annihilation of limit-cycle oscillations by identification of critical perturbing stimuli via mixed-integer optimal control," *Phys. Rev. Lett.*, vol. 95, no. 10, p. 108303, Sep. 2005.

[5] M. Engelhart, D. Lebiedz, and S. Sager, "Optimal control for selected cancer chemotherapy ode models: A view on the potential of optimal schedules and choice of objective function," *Math. Biosci.*, vol. 229, no. 1, pp. 123–134, Jan. 2011.

[6] A. Raue *et al.*, "Lessons learned from quantitative dynamical modeling in systems biology," *PLoS ONE*, vol. 8, no. 9, p. e74335, 2013.

[7] R. Heinrich, B. G. Neel, and T. A. Rapoport, "Mathematical models of protein kinase signal transduction," *Molecular Cell*, vol. 9, no. 5, pp. 957–970, 2002.

[8] C. Kreutz, A. Raue, D. Kaschek, and J. Timmer, "Profile likelihood in systems biology," *FEBS J.*, vol. 280, no. 11, pp. 2564–2571, Jun. 2013.

[9] A. Raue, C. Kreutz, T. Maiwald, J. Bachmann, M. Schilling, U. Klingmüller, and J. Timmer, "Structural and practical identifiability analysis of partially observed dynamical models by exploiting the profile likelihood," *Bioinformatics*, vol. 25, no. 15, pp. 1923–1929, 2009.

[10] K. P. Burnham and D. R. Anderson, *Model Selection Multimodel Inference: A Practical Information-Theoretic Approach*. New York, NY, USA: Springer, 2002.

[11] D. Kaschek and J. Timmer, "A variational approach to parameter estimation in ordinary differential equations," *BMC Syst. Biol.*, vol. 6, no. 1, p. 99, 2012.

[12] M. Braun, "trustOptim: An R package for trust region optimization with sparse Hessians," *J. Statist. Softw.*, vol. 60, no. 4, pp. 1–16, 2014. [Online]. Available: http://www.jstatsoft.org/v60/i04/

[13] F. Henjes *et al.*, "Strong EGFR signaling in cell line models of ERBB2-amplified breast cancer attenuates response towards ERBB2-targeting drugs," *Oncogenesis*, vol. 1, no. 7, p. e16, 2012.

[14] D. Kaschek, F. Henjes, M. Hasmann, U. Korf, and J. Timmer. (2015). *Supplement: Resolving the Pattern of AKT Activation by Variational Parameter Estimation*. [Online]. Available: http://jeti.uni-freiburg.de/papers/supplement_mTOR_IE_kaschek.pdf